Catalysis Today 175 (2011) 411–419

Contents lists available at ScienceDirect

Catalysis Today

journal homepage: www.elsevier.com/locate/cattod

# Preferential oxidation of CO in $H_2$ rich stream (PROX) over gold catalysts supported on doped ceria: Effect of water and $CO_2$

Lyuba Ilieva [a,*], Giuseppe Pantaleo [b], Ivan Ivanov [a], Rodolfo Zanella [c], Janusz W. Sobczak [d], Wojciech Lisowski [d], Anna Maria Venezia [b], Donka Andreeva [a]

[a] Institute of Catalysis, Bulgarian Academy of Sciences, "Acad. G. Bonchev" Str., bl. 11, 1113 Sofia, Bulgaria
[b] Istituto per lo Studio di Materiali Nanostrutturati, CNR, I-90146 Palermo, Italy
[c] Centro de Ciencias Aplicadas y Desarrollo Tecnológico, Universidad Nacional Autónoma de México, Circuito Exterior S/N, Ciudad Universitaria, C.P. 04510 México, D.F., Mexico
[d] Institute of Physical Chemistry, PAS, Kasprzaka 44/52, 01-224 Warszawa, Poland

ARTICLE INFO

*Article history:*
Received 20 October 2010
Received in revised form 5 May 2011
Accepted 24 May 2011
Available online 31 July 2011

*Keywords:*
PROX
Effect of water and $CO_2$
Gold
Ceria modified with $FeO_x$ or $MnO_x$

ABSTRACT

Gold catalysts on mechanochemically prepared mixed ceria supports doped with $FeO_x$ and $MnO_x$ were studied in the reaction of preferential oxidation of CO in $H_2$ rich stream (PROX) in the presence of 20% $CO_2$ and 10% $H_2O$. The average size and the size distribution of gold particles were estimated by HRTEM. By means of XPS the Au XPS states at various binding energies, assigned to differently charged Au nanoparticles, were distinguished. The catalytic activity and selectivity in the oxidation of CO in dry $H_2$-reach stream was high, however the PROX activity was significantly suppressed by the addition of high concentrations of water and $CO_2$. The two step calcinations of catalysts, first at 400 °C and then at 550 °C, showed no better performance in PROX reaction carried out at realistic experimental conditions. However, after the two-step calcination procedure, nanosized gold particles of high thermal stability were obtained over $MnO_x$ doped ceria.



## 1. Introduction

Catalytic conversion of organic fuel is one of the widely applied methods of hydrogen production. This process is usually followed by WGS reaction in order to minimize the residual CO concentration levels from 10–15% to nearly 1%. To prevent poisoning of the fuel cells anodes, the CO amount in hydrogen must be below 10 ppm for Pt anodes and below 100 ppm for CO-tolerant alloy anodes. Oxide-supported gold catalysts have been suggested as suitable candidates for lowering the level of CO concentration in hydrogen-rich stream via preferential oxidation of CO (PROX) [1]. This process is carried out in the temperature interval 80–100 °C, in which the gold based catalysts exhibit good activity and selectivity. Promising results in PROX have been obtained with gold supported on oxygen supplying supports as undoped and doped $CeO_2$ [2–4], $Fe_2O_3$ [5–9], $MnO_x$ [10,11] and $MnO_x$–$CeO_2$ [12] using dry $CO/H_2$ mixture. There is consensus of opinion that the presence of small gold nanoparticles is a pre-requisite for a high catalytic activity of this type of catalysts. The support composition not only affects the growth of gold particles but also the ability of supplying reactive oxygen species. Very recently, the study of $Au/CeO_2$–$Fe_2O_3$ catalysts confirmed this supposition showing that the variation of the support composition led to significant differences in the gold particles size and CO oxidation activity under PROX conditions [13]. At real conditions $CO_2$ and moisture are also present as side products in the reformate stream. PROX catalysts for practical application have to be capable of removing trace amounts of CO from excess of humid $H_2$ containing significant quantities of $CO_2$. The usual $CO_2$ concentration in the real reaction stream is about 20% and the $H_2O$ amount is about 10%. Sanchez et al. [10] have proposed supported gold as a promising PROX catalyst stating that the catalytic activity of Au is enhanced by moisture and almost insensitive to $CO_2$. Later studies have shown a negative effect of $CO_2$ on PROX activity and selectivity. Luengnaruemitchai et al. [14] have observed that the increasing of $CO_2$ concentration from 2 to 20% at reaction temperature of 380 K, reduced the PROX activity of $Au/CeO_2$ catalyst (from about 80% up to about 20%) but the selectivity was not significantly affected (~60%). $Au/MnO_x$ and $Au/FeO_x$ catalyst could resist up to 10% $H_2O$ in the reactant feed while their activities were suppressed in the presence of 20% $CO_2$ [15]. Panzera et al. [16] have shown that both CO conversion and selectivity over uncalcined and calcined $Au/CeO_2$ decreased as the $CO_2$ concentration increased, however for $CO_2$ concentration higher than 12% (where the conversion is lower than 20%), $CO_2$ affected slightly the CO conversion. Avgouropoulos et al. have reported the effect of $CO_2$ on activity and selectivity is negative (being more significant for undoped

* Corresponding author. Tel.: +359 29792572; fax: +359 29712967.
*E-mail address:* luilieva@ic.bas.bg (L. Ilieva).

0920-5861/$ – see front matter © 2011 Elsevier B.V. All rights reserved.
doi:10.1016/j.cattod.2011.05.041

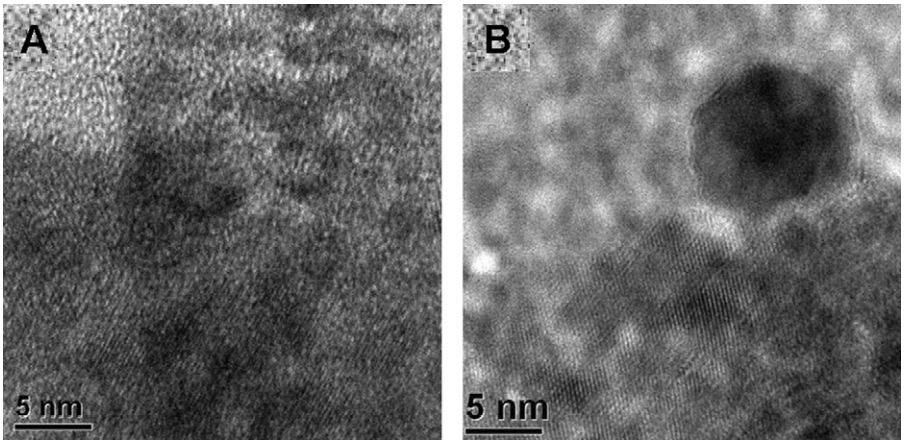


**Fig. 1.** HRTEM images of Fe-containing gold catalysts: (A) AuCeFeMA(400) sample and (B) AuCeFeMA(550) sample.

$Au/CeO_2$), while the presence of water improved the catalytic performance especially in the case of doped ceria catalysts. The Zn- and Sm-doped catalysts were found by the authors as the most resistant toward deactivation by $CO_2$ [17]. The deactivation of $Fe_2O_3$ supported gold catalysts caused by $CO_2$ and the beneficial influence of water on CO oxidation has been reported [18,19]. In Ref. [13] Tabakova et al. have observed that the atomic ratio Fe/(Ce + Fe) = 0.5 in the mixed oxides support of gold, prepared by co-precipitation, improves the resistance toward $CO_2$. On one hand the negative role of $CO_2$ could be ascribed to the competitive adsorption of $CO_2$ and CO (and $H_2$). The accumulation of carbonate and carboxylate species blocking the active sites [9,15] is depending on the nature of the support and the acidic supports were found to be more resistant to deactivation by $CO_2$ than the basic ones [20]. On the other hand the reverse water gas shift reaction (RWGS) between $CO_2$ and $H_2$ could occur, leading to the CO formation, thereby the target CO conversion cannot be reached. In order to achieve target activity and selectivity for the competitive oxidation of dilute CO in the excess of moist $H_2$ containing $CO_2$, an interesting proposal for suppressing the RWGS activity was the two-stage calcination procedure of $Au/Fe_2O_3$ catalyst [21]. Regarding the effect of water on the PROX activity and selectivity different observations have been reported. No retardation of the activity of CO oxidation in $H_2$-rich gas by the presence of $H_2O$ vapor over $Au/Fe_2O_3$ has been observed by Kahlich et al. [6]. Luengnaruemitchai et al. [14] have shown a lowering of the CO conversion over $Au/CeO_2$ under the humidified conditions at temperatures below 373 K but water was even favorable to the catalyst activity at high temperatures; the selectivity was slightly affected by the presence of water. The prevailing opinion about a positive influence of water is assigned to hydroxyl group formation, which is necessary for CO oxidation [22,23], or to enhancing the rate of carbonates decomposition via thermally less stable bicarbonate species [19,24]. According to a mechanism proposed by Bond and Thompson [25] water and hydroxyl groups play crucial role in facilitation of CO oxidation through the formation of the COOH intermediate groups. The same authors [26] commented the important role of water in preventing the formation of toxic inhibitors, such as $CO_3^{2-}$ and $HCO_3^-$, or removing them once they are formed.

Gold catalysts on mechanochemically prepared mixed ceria supports doped with $FeO_x$ and $MnO_x$ have been selected as the most promising catalyst for PROX among the recently studied gold catalysts on modified ceria synthesized by co-precipitation or mechanochemical activation [27]. The goal of the present investigation is to study the influence of moisture and $CO_2$ on the catalytic activity and selectivity of CO oxidation in PROX over these selected catalysts. $H_2$–CO stream containing 10% $H_2O$ and 20% $CO_2$, as usually applied at real reaction conditions, was chosen.

## 2. Experimental

The doped ceria supports were synthesized by mechanochemical activation (MA) using a freshly prepared vacuum-dried cerium hydroxide and the metal oxide dopant: $Fe_2O_3$ or $MnO_2$. The cerium hydroxide was obtained by precipitation of cerium nitrate with a solution of $K_2CO_3$. A mixture of cerium hydroxide and the corresponding amount of dopant was subjected to mechanochemical activation by milling for 30 min in a mortar and calcination at 400 °C for 2 h. Before deposition of gold hydroxide, the modified ceria support was activated in Ultrasonic UD-20 automatic UV disintegrator under vigorous stirring. The amount of dopant oxide was 10 wt%.

Gold was added by deposition–precipitation method. It was loaded as $Au(OH)_3$ on the corresponding modified ceria support, preliminary suspended in water, through the precipitation of $HAuCl_4{\cdot}3H_2O$ by $K_2CO_3$ under continuous stirring at constant pH = 7.0 and temperature of 60 °C. After 1 h of aging, filtering and careful washing, the precursors were dried under vacuum at 80 °C and calcined in air at 400 °C for 2 h. The obtained gold catalysts were denoted as AuCeFeMA(400) and AuCeMnMA(400). A portion of these samples underwent an additional calcination step at 550 °C for 2 h. The catalysts obtained after this two stage calcination, were denoted as AuCeFeMA(550) and AuCeMnMA(550). The amount of gold was 2 wt%. The syntheses were carried out in a Contalab system under full control of all parameters of preparation. The initial salts used were "analytical grade".

The BET surface area, XRD and TPR measurements with AuCeFeMA and AuCeMnMA catalysts have been described in a previous study [27].

High resolution transmission electron microscopy (HRTEM) and high angle annular dark field (HAADF) observations of Fe- and Mn-containing gold catalysts calcined at 400 °C and at 550 °C were performed in a JEM 2010 FasTem analytical microscope equipped with a Z-contrast annular detector. The histograms of the metal particle sizes were established from the measurement of more than 700 particles obtained by Z-contrast and thermal diffuse scattering (TDS) observations.

The X-ray photoelectron spectroscopy (XPS) data were recorded on a PHI 5000 VersaProbe scanning ESCA Microprobe using monochromatic Al Kα radiation ($h\nu$ = 1486.6 eV) from an X-ray source operating at 200 μm spotsize, 50 W and 15 kV. The analyzer pass energy was 23.5 eV, the electron take off angle was 80° and the energy step size was 0.05 eV for Au 4f XPS spectra and 0.1 eV for other elements. The samples containing Fe were additionally analyzed using the conventional Mg X-ray source (Kα radiation $h\nu$ = 1253.6 eV) operating at 300 W and 15 kV. Prior to analysis the samples were pressed into thin wafers and preliminary degassed

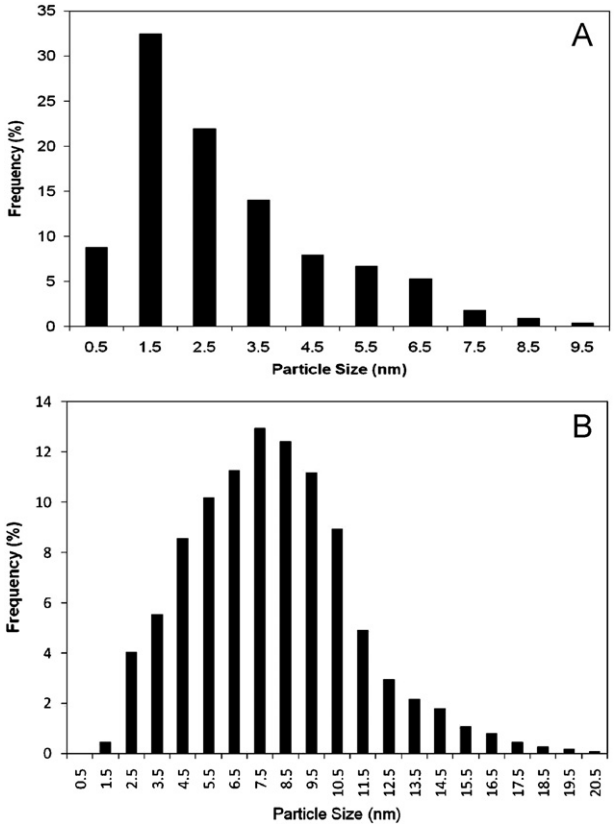


**Fig. 2.** Size distribution of gold particles in (A) AuCeFeMA(400) sample and (B) AuCeFeMA(550) sample.

in a preparation chamber. The Shirley background subtraction and peak fitting with Gaussian–Lorentzian product peak was performed using a XPS processing program Avantage (Thermo Electron Corporation) The charging effects were corrected by adjusting Ce $3d_{3/2}$ peak, usually described as u''' peak to a position of 917.00 eV [28]. This is a strong, individual peak and its position can be established much more precisely than that of the commonly used C 1s peak from adventitious carbon.

The catalytic activity and selectivity measurements in PROX were carried out using a quartz glass U-shaped reactor, equipped with a temperature programmed controller. Before the catalytic tests, the samples were treated in a flow of $O_2$ (5 vol%) in Ar during 30 min at 150 °C. The catalytic behaviour of AuCeFeMA(400) and AuCeMnMA(400) catalysts were compared using different gas feed composition: (route (i)) 50% $H_2$ + 0.3% CO + 0.3% $O_2$ (He as balance) and (route (ii)) 50% $H_2$ + 0.3% CO + 0.3% $O_2$ + 10% $H_2O$ + 20% $CO_2$ (He as balance). Experiments with gas mixture 50% $H_2$ + 0.3% CO + 0.3% $O_2$ + 5% $H_2O$ (He as balance) were also carried out. The AuCeFeMA(550) and AuCeMnMA(550) samples were tested applying route (ii). The total gas flow was 50 mL $min^{-1}$ corresponding to WHSV of 60,000 mL $g^{-1}$ $h^{-1}$. The CO conversion and the selectivity were calculated using an ABB infrared analyzer detector for CO and $CO_2$ and a ABB paramagnetic Magnos206 for the $O_2$. The converted CO was calculated on the basis of the $CO_2$ produced whereas the selectivity was estimated according to the following equation:

$$S(\%) = \frac{\text{ppm}\ \ CO_2^{out}}{2 \times (\text{ppm}\ \ O_2^{in} - \text{ppm}\ \ O_2^{out})} \times 100$$

## 3. Results and discussion

The characterization of AuCeFeMA(400) and AuCeMnMA(400) catalysts by means of XRD and TPR measurements are given in details in Ref. [27]. The estimate by XRD average particle sizes of ceria for both catalysts were of the same order: 10.1 nm and 10.7 nm for samples doped by Fe and Mn, respectively. The XRD spectra showed lines typical of fluorite type structure of ceria, in addition $Fe_3O_4$ phase was registered with AuCeFeMA(400) catalyst. In addition to the XRD data of AuCeMnMA(400) sample showed highly dispersed Au phase as well as the presence of gold particles with low dispersion, however having a very little impact onto the overall surface of gold: 1 large crystallite of 25 nm per 20,000 crystallites of 2.9 nm.

Taking into account the hydrogen consumption in the TPR experiments and the stoichiometry of the reduction processes, the presence of $Fe_2O_3$ and $Fe_3O_4$ in AuCeFeMA(400) catalyst as well as $MnO_2$ and $Mn_2O_3$ in AuCeMnMA(400) sample has been deduced [27]. The careful analysis of the HRTEM images of both catalysts prepared by MA confirms the existence of $Fe_2O_3$ and $Fe_3O_4$ in the Fe doped catalysts as well as $MnO_2$ and $Mn_2O_3$ in the catalysts containing Mn [27].

Fig. 1 shows the HRTEM images of the Fe-containing gold catalyst calcinated at 400 °C and then at 550 °C. The gold particle size distribution, as determined using HAADF (Z-contrast) method, is presented in Fig. 2. Figs. 3 and 4 show the corresponding TEM data for the AuCeMnMA(400) and AuCeMnMA(550) catalysts. It is seen that the size distribution of gold particles in the AuCeFeMA(400) sample is similar to AuCeMnMA(400) one exhibiting the relatively

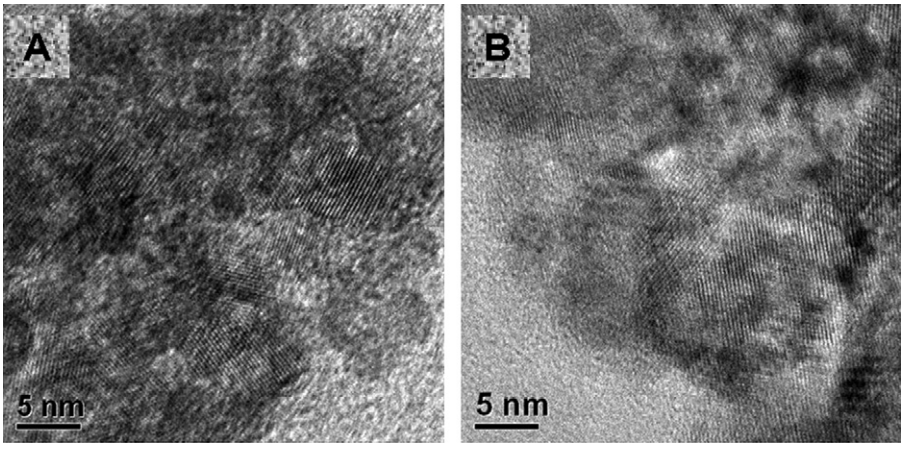


**Fig. 3.** HRTEM of Mn-containing gold catalysts: (A) AuCeMnMA(400) sample and (B) AuCeMnMA(550) sample.

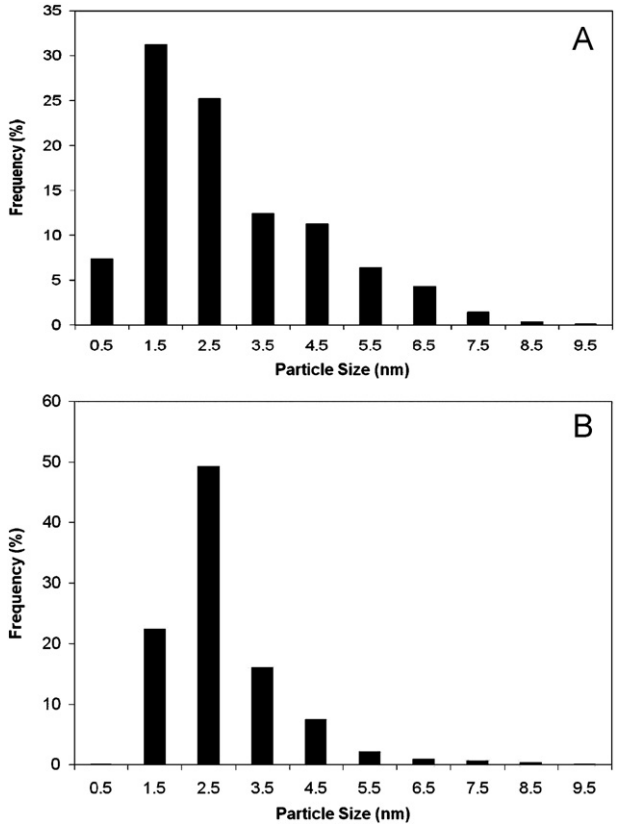


**Fig. 4.** Size distribution of gold particles in (A) AuCeMnMA(400) sample and (B) AuCeMnMA(550) sample.

highest number of particles with size of 1.5 and 2.5 nm. The calculated average size of gold particles is 2.9 nm for both samples.

The second step of calcinations, performed at 550 °C, influenced the dispersion of gold on Fe-doped catalyst in different way than on Mn-doped sample. High contribution of large size gold particles has been observed in the AuCeFeMA(550) as a result of small gold particles agglomeration. The fraction of very small particles of 0.5 nm disappeared and the amount of particles of 1.5 and 2.5 nm was much lower than in the AuCeFeMA(400) sample (see Fig. 2). The average particle size of gold in AuCeFeMA(550) is 8.0 nm, however the size distribution is very large, some big particles of more than 15 nm are observed (Fig. 2B). Quite different modification of dispersed Au phase can be observed for the AuCeMnMA(550) sample. The amount of particles larger than 3.5 nm becomes lower after the higher temperature calcinations and the fraction of particles with size of 2.5 nm is a dominant part of Au phase. As the amount of very small particles (0.5 and 1.5 nm) also decreases, the average particles size of gold for AuCeMnMA(550) is 2.8 nm, practically the same as that for AuCeMnMA(400) sample.

The data calculated from the XPS measurements of the studied fresh AuCeFeMA(400) and AuCeMnMA(400) catalysts as well as of the fresh and spent (following route (ii)) AuCeFeMA(550) and AuCeMnMA(550) samples are summarized in Table 1. The Au 4f XPS spectra of the corresponding fresh and spent samples are illustrated in Fig. 5 – for Fe-containing gold catalysts in left column and for Mn-containing gold catalysts in right column, respectively. Following the XPS peak fitting analysis of the Au 4f XPS spectra of all studied samples one can distinguish the Au XPS states at various binding energies (BE), which can be assigned to differently charged Au nanoparticles. Both electronegative ($Au^{\delta-}$) and electropositive ($Au^{\delta+}$) oxidation states of gold in addition to metallic gold ($Au^0$) can be distinguished. The analysis of AuCeFeMA(400) and AuCeMnMA(400) fresh samples showed the $Au^{\delta+}$ oxidation states (BE higher than 84.2 eV) to be the dominant part of the gold in addition to metallic gold (BE equal to 84.0 ± 0.2 eV). For the AuCeMnMA(400) sample also a small amount of $Au^{\delta-}$ oxidation state (BE lower than 83.8 eV) has been detected. The XPS spectra collected for fresh samples calcined at 550 °C revealed relatively higher contribution of metallic gold as compared with the corresponding fresh samples calcined at 400 °C. The second step of calcination also strongly affects the Ce 3d spectra for both catalysts (see Fig. 6) making these spectra more complex. This is an open question whether this spectra modification is caused only by high temperature treatment or we observe an additional Ce 3d states arising as a result of cerium oxide interaction with Mn- and Fe-dopant. In order to make this point more clear we analyzed additionally the AuCe specimens calcined at 400 °C and 550 °C, respectively. In this way we could observe separately the high-temperature treatment effect excluding the metal (Me)-dopant interaction. Indeed the Ce 3d XPS

**Table 1**
Au $4f_{7/2}$ and Me $2p_{3/2}$ BE (Me = Mn or Fe), along with their percentages for gold catalysts: fresh and after the catalytic operation following route (ii).

| Sample | Au $4f_{7/2}$ | | | | Me | Me $2p_{3/2}$ | Me% |
|---|---|---|---|---|---|---|---|
| | BE (eV) | at% | Au% | State | | BE (eV) | |
| AuCeMnMA(400) fresh | 86.11 | 0.03 | 18.67 | $Au^{3+}$ | | | |
| | 85.14 | 0.07 | 39.34 | $Au^{1+}$ | | | |
| | 83.98 | 0.07 | 37.30 | $Au_{met}$ | $Mn^{4+}$ | 643.05 | 46.1 |
| | 82.15 | 0.01 | 4.69 | $Au^{\delta-}$ | $Mn^{3+}$ | 641.50 | 53.9 |
| AuCeFeMA(400) fresh | 85.79 | 0.04 | 19.05 | $Au^{1+}$ | | | |
| | 84.87 | 0.12 | 56.17 | $Au_{small\ clusters}$ | $Fe^{3+}$ | 711.54 | 53.4 |
| | 84.00 | 0.05 | 24.77 | $Au_{met}$ | $Fe^{2+}$ | 710.09 | 46.6 |
| AuCeMnMA(550) fresh | 86.39 | 0.01 | 5.76 | $Au^{3+}$ | | | |
| | 85.13 | 0.05 | 36.63 | $Au^{1+}$ | | | |
| | 84.88 | 0.02 | 13.35 | $Au_{small\ clusters}$ | $Mn^{4+}$ | 642.30 | 65.2 |
| | 84.00 | 0.06 | 44.26 | $Au_{met}$ | $Mn^{3+}$ | 640.75 | 34.8 |
| AuCeFeMA(550) fresh | 85.12 | 0.07 | 52.02 | $Au^{1+}$ | $Fe^{3+}$ | 712.17 | 27.3 |
| | 84.00 | 0.06 | 47.98 | $Au_{met}$ | $Fe^{2+}$ | 710.62 | 72.7 |
| AuCeMnMA(550) spent | 85.36 | 0.03 | 26.15 | $Au^{1+}$ | | | |
| | 84.33 | 0.07 | 52.01 | $Au_{small\ clusters}$ | $Mn^{4+}$ | 642.53 | 71.3 |
| | 84.00 | 0.03 | 21.84 | $Au_{met}$ | $Mn^{3+}$ | 640.98 | 28.7 |
| AuCeFeMA(550) spent | 85.87 | 0.01 | 13.88 | $Au^{1+}$ | | | |
| | 84.43 | 0.04 | 52.43 | $Au_{small\ clusters}$ | $Fe^{3+}$ | 711.86 | 38.4 |
| | 84.00 | 0.03 | 33.70 | $Au_{met}$ | $Fe^{2+}$ | 710.41 | 61.6 |

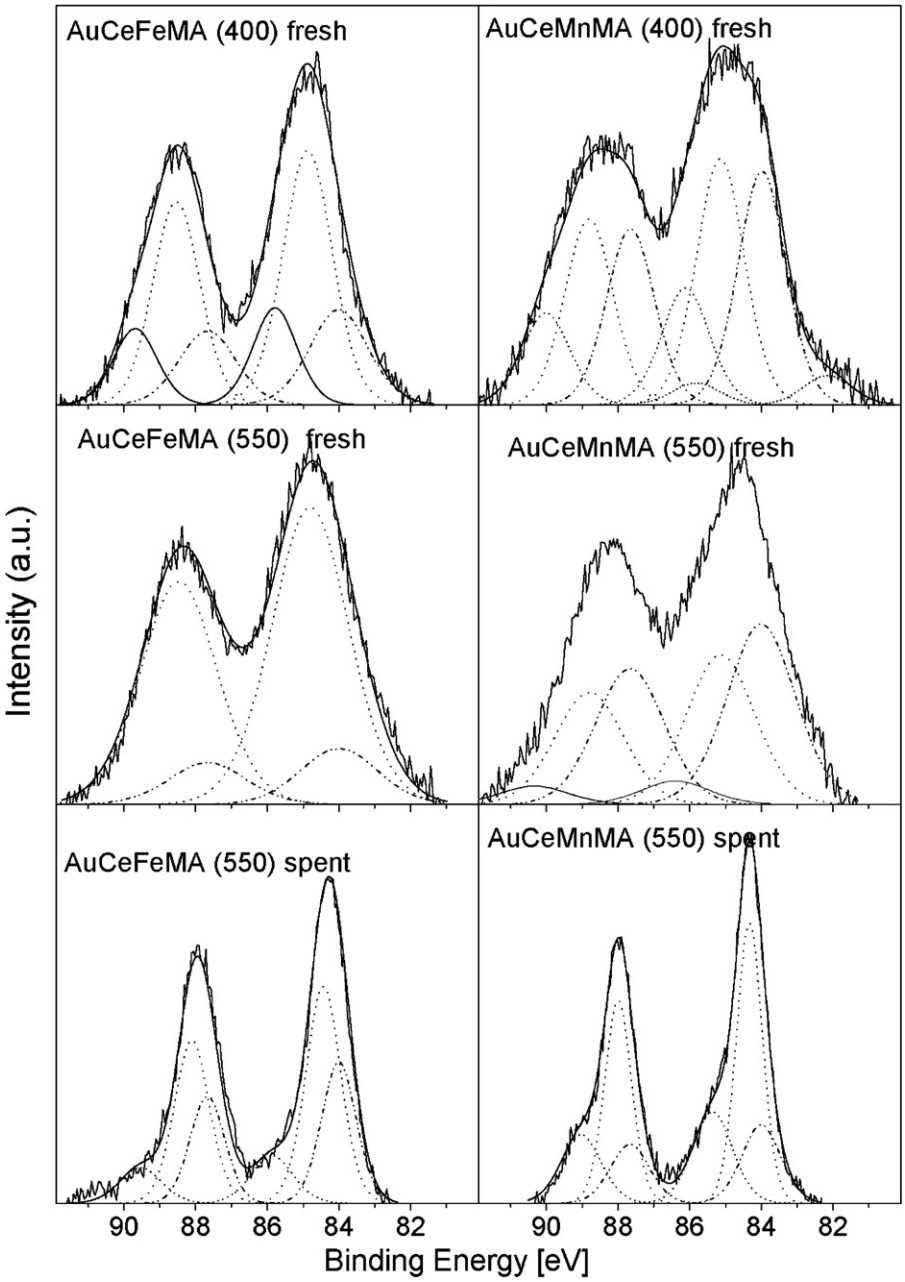


**Fig. 5.** Experimental and fitted Au 4f XPS spectra of Fe (left column) and Mn (right column) containing gold catalysts: fresh, after one- and two-steps calcinations, and spent after catalytic processing following the experimental route (ii).

spectra presented in Fig. 7 revealed some features being different after calcinations at 400 °C and 550 °C, respectively. However these effects are not as distinct as we observed for the catalysts with Me-dopant (compare Ce 3d spectra in Fig. 6). Thus it is likely that high-temperature interaction of Me-dopants can also influence the cerium oxide phase.

The XPS analysis reveals also a complex chemical nature of Me-oxide dopants in all calcined samples. $MnO_2$ and $Mn_3O_4$ were found to be coexisting Mn-phases in both Mn-containing samples calcined at 400 °C and 550 °C, respectively. Fe-containing samples show $Fe_2O_3$ and $Fe_3O_4$ to be present in both calcined samples.

The catalytic activity expressed as a degree of CO conversion and the selectivity toward $CO_2$ over Fe- and Mn-doped gold catalysts are shown in Figs. 8 and 9, respectively. Lines 1 illustrate the catalytic behaviour using gas feed (i): 50% $H_2$ + 0.3% CO + 0.3% $O_2$, lines 2 – using gas feed (ii): 50% $H_2$ + 0.3% CO + 0.3% $O_2$ + 10% $H_2O$ + 20% $CO_2$, and lines 3 – using gas feed (ii) over catalyst after the second step of calcination at 550 °C. Very high and stable activity (close to 100%) and a stable selectivity (about 40%) in the interval from the room temperature up to 200 °C were observed for AuCeFeMA(400) catalyst using dry CO–$H_2$ gas mixture (Fig. 8, curves 1). The corresponding AuCeMnMA catalyst, explored in the temperature interval, which is of interest for fuel cell application, exhibits 86% conversion of CO and 61% selectivity at 77 °C and 94% conversion and 39% selectivity at 100 °C, respectively (Fig. 9, curves 1). It is likely that this promising PROX behaviour is caused by the active centers with the participation of nanosized gold, formed on both ceria oxide support modified with Fe or Mn and on coexisting $FeO_x$ or $MnO_x$ phases. However, the reaction tests carried out at real conditions after adding 10% $H_2O$ and 20% $CO_2$ to the dry feed gas showed a significant drop in activity and selectivity with both gold catalysts. In the case of AuCeFeMA(400) sample (Fig. 8, curves

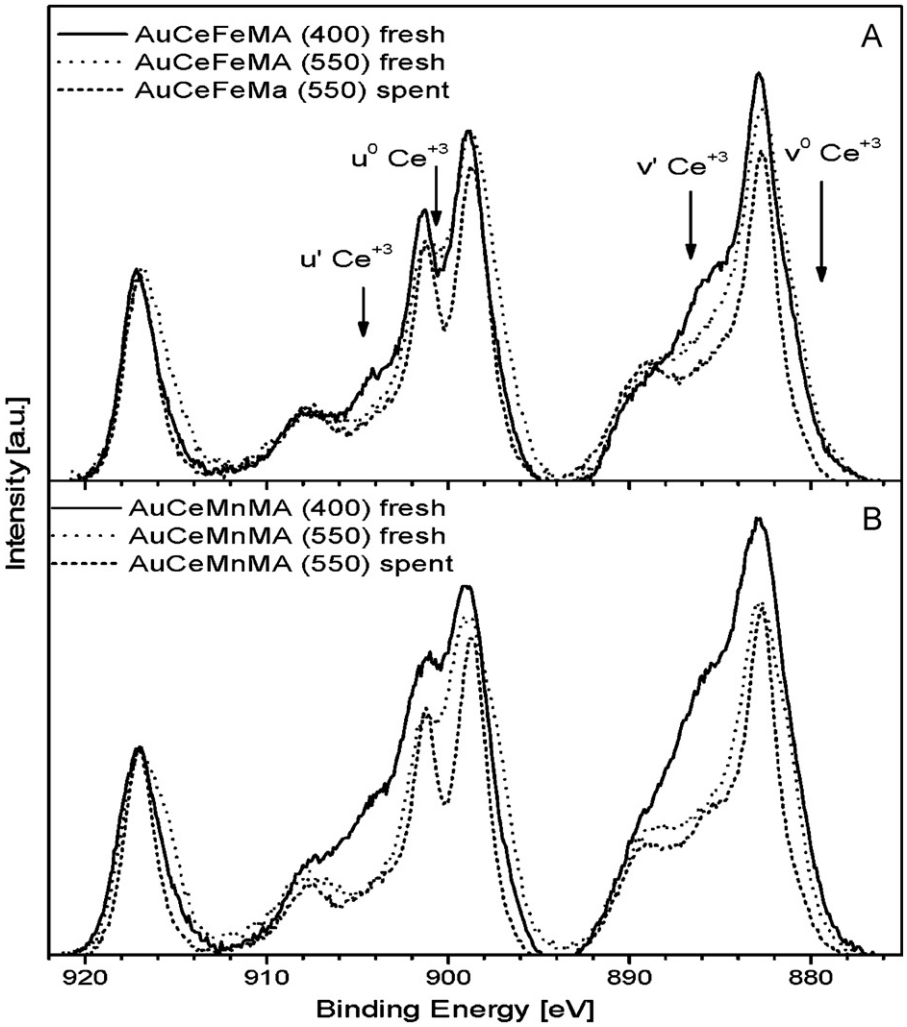


**Fig. 6.** Ce 3d XPS spectra of Fe (A) and Mn (B) containing gold catalysts: fresh after one- and two-steps calcinations, and spent after catalytic processing following the experimental route (ii).

2) the almost 100% CO conversion was reduced to less then 10% in the interval from room temperature to 77 °C, and to 15% at 100 °C, whereas 40% selectivity, which was stable from room temperature up to 150 °C, was lowered to about 20%. Using the AuCeMnMA(400) catalysts (Fig. 9, curves 2) the CO conversion decreased from 86% to only 7% at 77 °C and from 94% to 43% at 100 °C, respectively. The selectivity was lowered from 61% to 38% at 77 °C, and from 39% to 24% at 100 °C, respectively. The undesired reaction of CO methanation did not take place – during all experiments methane formation was not observed.

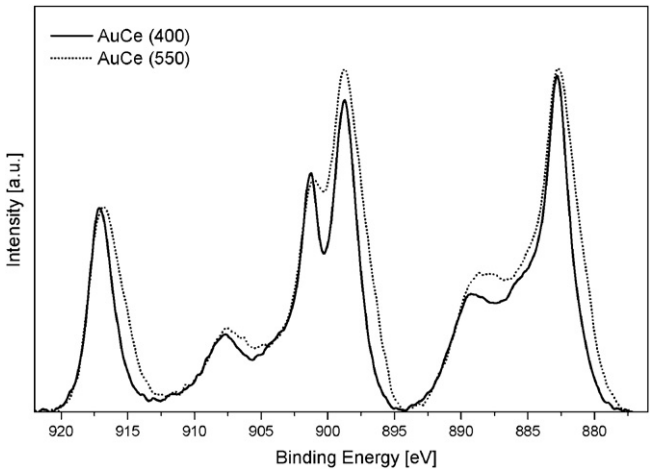


**Fig. 7.** Ce 3d XPS spectra of AuCe catalyst after calcination at 400 °C and 550 °C.

The influence of water on the catalytic activity in PROX has been examined adding $H_2O$ to the CO–$H_2$ mixture and a positive effect was expected on the basis of the role of water in the mechanism of CO oxidation, reported in the literature. The mechanism of Daniells et al. [29] was based on the model initially proposed by Bond and Thompson [25] and refined by Kung and co-workers [30,31]. The latter involves the insertion of an Au-bonded CO molecule into an $Au^+$–OH bond to form a hydroxycarbonyl. This species is oxidized to bicarbonate, which decomposes into $Au^+$–OH and $CO_2$. By reacting with poisoning carbonates, water would produce a hydroxyl and active bicarbonate, and thus regenerate the catalyst. Another alternative to the $CO_{ad} + O_{ad}$ model has been proposed by Date et al. [24], on the basis of experiments showing water-induced promotion of CO oxidation on several gold catalysts. In this mechanism the promotional role of water is for activation of oxygen and decomposition of carbonates. $O_{2ad}$ would react with $H_2O_{ad}$ at the gold particle periphery to form two hydroxyl groups and active oxygen, which is able to react with $CO_{ad}$ to form $CO_2$ via a carboxylate. However, the results obtained in the present investigation showed that the addition of water with concentration even lower (5%) than the

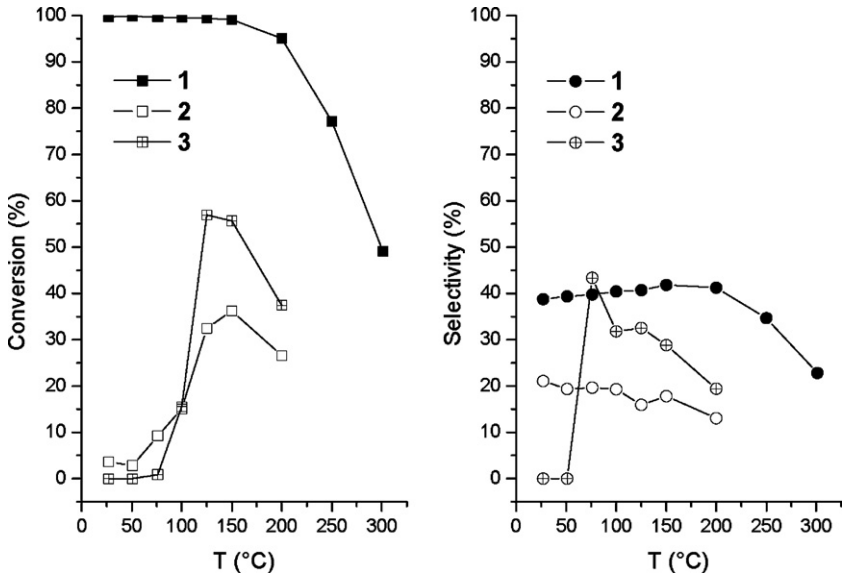


**Fig. 8.** Comparison regarding the degree of CO conversion and the selectivity over gold catalysts: curve lines 1 – AuCeFeMA(400) following route (i) with gas feed 50% $H_2$ + 0.3% CO + 0.3% $O_2$, curve lines 2 – AuCeFeMA(400) following route (ii) with gas feed 50% $H_2$ + 0.3% CO + 0.3% $O_2$ + 10% $H_2O$ + 20% $CO_2$, and curve lines 3 – AuCeFeMA(550) following route (ii).

usually existing in the reformate stream, does not improve the catalytic performance in PROX compared to dry feed gas interaction (see Figs. 10 and 11). The CO conversion, performed on the AuCeFeMA(400) catalysts at both RT and 50 °C, was suppressed from almost 100% to less than 15% in the presence of water (Fig. 10). In the interval 77–100 °C the CO conversion was lowered to 84% but the selectivity decreased only slightly. A small decrease of the CO conversion and the selectivity have been noted using AuCeMnMA(400) catalyst in the presence of moisture (Fig. 11). The absence of a positive influence of water and even the decreasing activity of CO oxidation could be explained by the existing in the literature opinion of blocking the active sites due to a strong adsorption [14,26]. Supplementary experiments performed with 20% $CO_2$ and 5% or 10% $H_2O$ in the feed showed insignificant changes of the CO conversion and selectivity for both water contents used (results not shown in figure).

High concentration of $CO_2$ drastically decreases the catalytic performance in PROX over both AuCeFeMA(400) and AuCeMnMA(400) catalysts. One negative influence of $CO_2$ addition is the blocking of active sites for CO adsorption. Other important negative effect is the back-formation of CO from $CO_2$ via the reverse water gas shift (RWGS) reaction: $CO_2 + H_2 \leftrightarrow CO + H_2O$. The minimization of the negative influence of $CO_2$ could be achieved lowering the activity of the catalyst for the RWGS reaction and retaining the CO oxidation activity. In respect to this purpose Landon et al. [21] proposed a preparation of 5 wt% Au on $Fe_2O_3$ including calcination at 400 °C, followed by calcination at 550 °C. After such two-steps calcination procedure (interestingly, the performance of the catalyst calcined directly at 550 °C did not reproduce that after the step calcination) a very high level of CO conversion (close to 100%) and selectivity (about 98%) was reported for PROX at 80 °C in the presence of 22% $CO_2$ and 4.7% $H_2O$ using

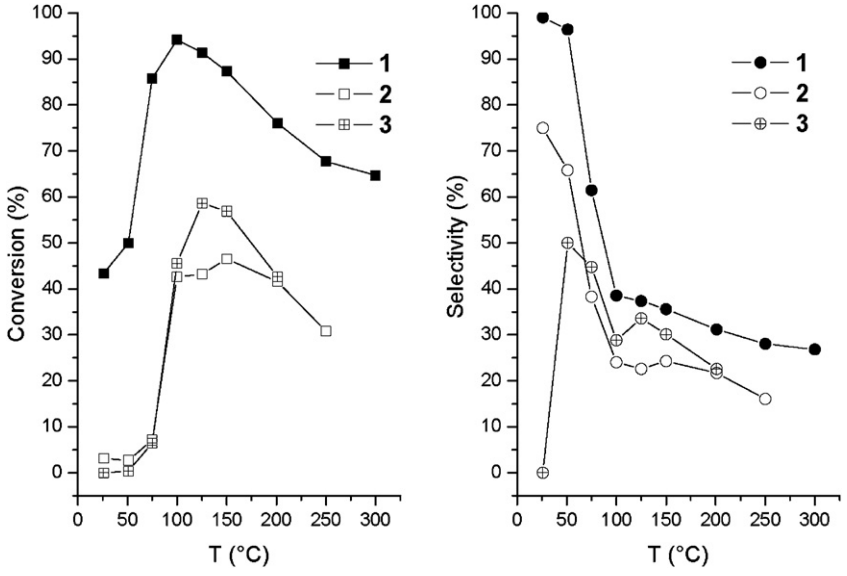


**Fig. 9.** Comparison regarding the degree of CO conversion and the selectivity over gold catalysts: curve lines 1 – AuCeMnMA(400) following route (i) with gas feed 50% $H_2$ + 0.3% CO + 0.3% $O_2$, curve lines 2 – AuCeMnMA(400) following route (ii) with gas feed 50% $H_2$ + 0.3% CO + 0.3% $O_2$ + 10% $H_2O$ + 20% $CO_2$, and curve lines 3 – AuCeMnMA(550) following route (ii).

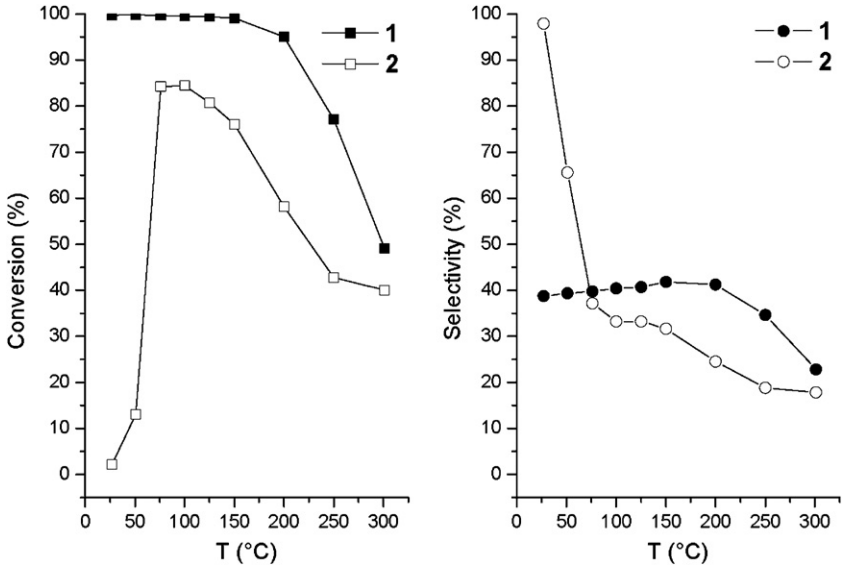


**Fig. 10.** Comparison regarding the degree of CO conversion and the selectivity over AuCeFeMA(400) catalyst: curve lines 1 – with gas feed 50% $H_2$ + 0.3% CO + 0.3% $O_2$ and curve lines 2 – with gas feed 50% $H_2$ + 0.3% CO + 0.3% $O_2$ + 5% $H_2O$.

GHSV = 12,000 $h^{-1}$. XPS analysis of catalysts processed in both consecutive steps of calcinations revealed cationic gold in the catalyst calcinated at 400 °C and only metallic gold after second stage of calcinations at 550 °C. On the basis of this results Landon et al. [21] elucidated the PROX results considering the metallic gold to be active for CO oxidation [32] and cationic gold to be particularly effective for WGS [33] and consequently for RWGS reaction. Having in mind these observations, AuCeFeMA(550) and AuCeMnMA(550) catalysts were prepared by calcination at 400 °C, then at 550 °C and a detailed characterization of the size and oxidation state of gold particles was performed. The catalytic results are presented in Figs. 8 and 9 (see curves 3). At 77 °C and above some improvement of the catalytic performance is seen, however the levels of CO conversion with dry $H_2$–CO mixture were far from being reached. The calcination at 550 °C leads to decrease of Au dispersion in AuCeFeMA(550) catalyst, while practically it did not caused a change in gold dispersion with AuCeMnMA(550) one (HRTEM results). Unlike the results reported in Ref. [21], the XPS data in the present study showed that the high temperature calcinations did not caused only metallic gold formation. Gold with higher BE, characteristic of partially positively charged particles exists (its part for AuCeMnMA(550) sample is bigger in agreement with the presence of higher amount of very small gold particles). The PROX reaction performed at real conditions implicates the transfer of electron density, in which gold and cerium as well as Fe- and Mn-dopants are involved. This was evidenced by careful analysis of the fresh and spent AuCeFeMA(550) and AuCeMnMA(550) catalysts using XPS technique. The Ce 3d XPS spectra of spent samples presented in Fig. 6 revealed lowering of the $Ce^{3+}$ ions concentration as compared with the corresponding fresh samples. Moreover, the relative concentration of Fe- and Mn-dopants of lower oxidation states as well as the relative concentration of metallic Au decrease after the PROX reaction processing (compare the XPS data in Table 1).

The dispersion of gold is a crucial factor affecting the both process – the desired CO oxidation and the undesired RWGS, the latter being more significant in the presence of high concentration of $CO_2$.

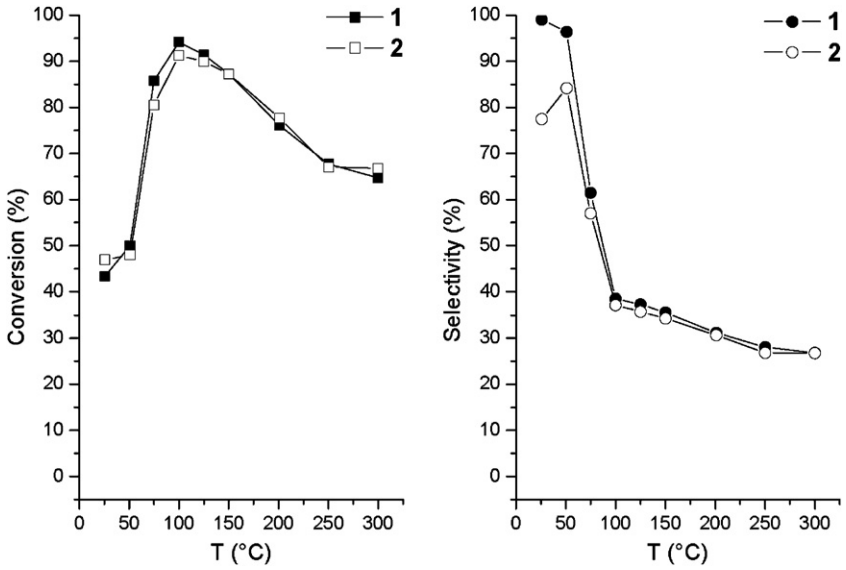


**Fig. 11.** Comparison regarding the degree of CO conversion and the selectivity over AuCeMnMA(400) catalyst: curve lines 1 – with gas feed 50% $H_2$ + 0.3% CO + 0.3% $O_2$ and curve lines 2 – with gas feed 50% $H_2$ + 0.3% CO + 0.3% $O_2$ + 5% $H_2O$.

A contradiction about the role of metallic or positively charged gold particles for WGS (respectively RWGS) exists in the literature. In our previous studies of gold/ceria catalysts, $Au^{\delta+}V_oCe^{3+}$ were proposed as active sites in the WGS reaction ($V_o$ is an oxygen vacancy) [34–36] which is in agreement with the supposition of Landon et al. [21] that the cationic gold is particularly effective for RWGS. By the analogy with the results in Ref. [20], a positive effect of two steps calcination procedure, connected to metallic gold formation and suppressing of the RWGS, was expected. However, the lowering of the negative effect of RWGS was not achieved. The gold particles on Fe- and especially Mn-modified ceria kept their $Au^{\delta+}$ state even after the high temperature treatment.

## 4. Conclusions

Mechanochemically prepared gold catalysts supported on ceria doped with $FeO_x$ and $MnO_x$ exhibit high activity and selectivity in preferential oxidation (PROX) of CO in dry $H_2$-reach stream. The PROX activity is significantly suppressed by high concentrations of $CO_2$ and water. The two step calcinations of catalysts, first at 400 °C and then at 550 °C, showed no better performance in PROX reaction carried out in realistic experimental conditions. However, after the two-step calcination procedure, nanosized gold particles of high thermal stability were obtained over $MnO_x$ doped ceria.

## Acknowledgments

This research study has been performed in the framework of a D36/003/06 COST program. L.I., I.I., A.M. and D.A. gratefully acknowledge the support provided by the National Science Fund, Ministry of Education and Sciences of Bulgaria (project TK-X-1709). The Bulgarian, Italian and Polish teams also indebted to the bilateral collaboration supported by CNR, respectively Polish Academy of Science, and Bulgarian Academy of Science. R.Z. acknowledges PUNTA (IMPULSA 01), PAPIIT IN108310 and CONACYT 55154 project for the financial support.

## References

[1] D. Cameron, R. Holliday, D. Thompson, J. Power Sources 118 (2003) 298, and references therein.
[2] O. Goerke, P. Pfeifer, K. Shubert, Appl. Catal. A 263 (2004) 11.
[3] F. Arena, P. Famulari, G. Trunfio, G. Bonura, F. Frusteri, L. Spadaro, Appl. Catal. B 66 (2006) 81.
[4] L. Ilieva, G. Pantaleo, I. Ivanov, R. Zanella, A.M. Venezia, D. Andreeva, Int. J. Hydrogen Energy 34 (2009) 6505.
[5] M.M. Shubert, S. Hackenberg, A.C. van Veen, M. Muhter, V. Pizak, R.J. Behm, J. Catal. 197 (2001) 113.
[6] M.J. Kahlich, H.A. Gasteiger, R.J. Behm, J. Catal. 182 (1999) 430.
[7] S. Scire, C. Crisafulli, S. Minico, G.G. Condorelli, A. Di Mauro, J. Mol. Catal. A: Chem. 284 (2008) 24.
[8] H. Imai, S. Date, S. Tsubota, Catal. Lett. 124 (2008) 68.
[9] M.M. Schubert, V. Pizak, J. Garche, R.J. Behm, Catal. Lett. 76 (2001) 143.
[10] R.M.T. Sanchez, A. Ueda, K. Tanaka, M. Haruta, J. Catal. 168 (1997) 125.
[11] L.-C. Wang, X.-S. Huang, Q. Liu, Y.-M. Liu, Y. Cao, H.-Y. He, K.-N. Fan, J.-H. Zhuang, J. Catal. 259 (2008) 66.
[12] L.-H. Chang, N. Sasirekha, B. Rajesh, Y.-W. Chen, W.-J. Wang, Ind. Eng. Chem. Res. 45 (2006) 4927.
[13] T. Tabakova, G. Avgouropoulos, J. Papavasiliou, M. Manzoli, F. Boccuzzi, K. Tenchev, F. Vindigni, T. Ioannides, Appl. Catal. B: Environ. 101 (2011) 256.
[14] A. Luengnaruemitchai, S. Osuwan, E. Gulari, Int. J. Hydrogen Energy 29 (2004) 429.
[15] A. Luengnaruemitchai, D.T.K. Thoa, S. Osuwan, E. Gulari, Int. J. Hydrogen Energy 30 (2005) 981.
[16] G. Panzera, V. Modafferi, S. Candamano, A. Donato, F. Rusteri, P.L. Antonucci, J. Power Sources 135 (2004) 177.
[17] G. Avgouropoulos, M. Manzoli, F. Boccuzzi, T. Tabakova, J. Papavasiliou, T. Ioannides, V. Idakiev, J. Catal. 256 (2008) 237.
[18] G. Avgouropoulos, T. Ionnides, C. Papadopoulou, J. Batista, S. Hocevar, H.K. Matralis, Catal. Today 75 (2002) 157.
[19] M.M. Schubert, A. Venugopal, M.J. Kahlich, V. Plzak, R.J. Behm, J. Catal. 222 (2004) 32, and references therein.
[20] G.C. Bond, D.T. Thompson, Catal. Rev. Sci. Eng. 41 (1999) 319.
[21] P. Landon, J. Ferguson, B.E. Solsona, T. Garcia, A.F. Carley, A.A. Herzing, C.J. Kiely, S.E. Golunski, G.J. Hutchings, Chem. Commun. (2005) 3385–3387.
[22] M. Haruta, S. Tsubota, T. Kobayashi, H. Kageyama, M.J. Genet, B. Delmon, J. Catal. 144 (1993) 175.
[23] G.Y. Wang, H.L. Lian, W.X. Zhang, D.Z. Jiang, T.H. Wu, Kinet. Catal. 43 (2002) 433.
[24] M. Date, M. Okumura, S. Tsubota, M. Haruta, Angew. Chem. Int. Ed. 43 (2004) 2129.
[25] G.C. Bond, D.T. Thompson, Gold Bull. 33 (2000) 41, and references therein.
[26] G.C. Bond, D.T. Thompson, Gold Bull. 42 (2009) 247, and references therein.
[27] L. Ilieva, G. Pantaleo, I. Ivanov, A. Maximova, R. Zanella, Z. Kaszkur, A.M. Venezia, D. Andreeva, Catal. Today 158 (2010) 44.
[28] L. Armelao, D. Barecca, G. Bottaro, A. Gasparotto, E. Tondello, Surf. Sci. Spectra 8 (2001) 247.
[29] S.T. Daniells, M. Makkee, J.A. Moulijn, Catal. Lett. 100 (2005) 39.
[30] M.C. Kung, R.J. Davis, H.H. Kung, J. Phys. Chem. C 111 (2007) 11767, and references therein.
[31] C.K. Costello, M.C. Kung, H.S. Oh, Y. Wang, H.H. Kung, Appl. Catal. A 232 (2002) 159.
[32] M.S. Chen, D.W. Goodman, Science 306 (2004) 252.
[33] Y. Liu, Q. Fu, M. Flytzani-Stephanopoulos, Catal. Today 241 (2004) 93.
[34] D. Andreeva, I. Ivanov, L. Ilieva, J.W. Sobczak, G. Avdeev, K. Petrov, Top. Catal. 44 (2007) 173.
[35] D. Andreeva, I. Ivanov, L. Ilieva, M.V. Abrashev, R. Zanella, J.W. Sobczak, W. Lisowski, M. Kancheva, G. Avdeev, K. Petrov, Appl. Catal. A 357 (2009) 159.
[36] D. Andreeva, M. Kantcheva, I. Ivanov, L. Ilieva, J.W. Sobczak, W. Lisowski, Catal. Today 158 (2010) 69.